task is necessary to transfer to the correct mode of operation. This processing requires under 2 ms to complete. Thus, the adaptive tracker processor can recover from an error reset to the previous mode of operation in under 20 ms.

References

[1] Kinnison, J. D. et al., "Radiation Characterization of the ADSP 2100A Digital Signal Processor," *IEEE Transactions in Nuclear Science*, Vol. NS-38, Dec. 1991, pp. 1398–1402.

[2] Nichols, D. K. et al., "Update on Parts SEE Susceptibility from Heavy Ions," *IEEE Transactions in Nuclear Science*, Vol. NS-38, Dec. 1991, pp. 1529–1539.

[3] Kinnison, J. D., McKerracher, P. L., Maurer, R. H., and Carkhuff, B. G., "Single Event Survivability of Unhardened VLSI Devices," *Proceedings of the 1990 Advanced Micro-electronics Technology Qualification, Reliability and Logistics Workshop*, San Diego, CA, Department of Defense Tri-Service MIMIC Qualification Committee, 1990, pp. 239–248.

[4] Spaur, C. W., "TOPEX Radar Altimeter Signal Processor SEU Recovery," Applied Physics Lab., S2F-890126, Laurel, MD, March 1989.

[5] Maurer, R. H., Kinnison, J. D., Romenesko, B. M., Carkhuff, B. G., and King, R. B., "Space Radiation Qualification of a Microprocessor Implemented for the Intel 80186," *Proceedings of the 2nd Annual AIAA/USU Conference on Small Satellites*, Center for Space Engineering, Utah State University, Logan, UT, Technical Session 111, Paper 3, 1988.

Perturbed Volume of Orbiting Debris

Joshua Ashenberg*
Chelmsford, Massachusetts 01863

Nomenclature

A = particle reference area
C_D = drag coefficient
$\boldsymbol{D}$ = atmospheric drag
H = density scale height
J_2 = second zonal harmonic of the Earth
m = particle mass
$\boldsymbol{r}$ = radius vector
R_E = Earth's radius
$\boldsymbol{V}$ = velocity
z = Earth's polar axis
ρ = atmospheric density
μ = geocentric gravitational constant

Introduction

THE common scenario of debris spread due to an orbital breakup consists of the following phases.' During the first phase, which lasts only few revolutions, the debris cloud forms a pulsating ellipsoid. An important feature is related to the constriction points, also named "pinch points"" at which the cloud is constricted in one or two dimensions. The other phases are the propagation of the cloud forming a torus-like shape, the zonal spread due to the Earth's oblateness? and finally, the "cleaning" due to the atmospheric drag. We will concentrate here on the first phase. For most of the applications, the unperturbed two-body dynamics is sufficient for dealing with the short term. However, for a more accurate prediction, especially concerning the constriction points, the inclusion of the perturbations is essential.

Our case study is the inclusion of the dominant perturbations in the propagation of particles after an isotropic explosion in low Earth orbits. We are mainly interested in the volume which is occupied by these particles. We deal here with the perturbations due to the Earth's oblateness (J_2) and due to the atmospheric drag. The method of solution is the linearized perturbations, which provides a first-order solution about the reference orbit. Regarding the set of coordinates, we prefer here the inertial frame of reference, rather than the orbital frame which is commonly used in problems related to relative motion.[6] Although the orbital frame provides us with an analytical solution? it is quite cumbersome when dealing with the linearized J_2 perturbations. Since the volume is invariant under translation or rotation, we expect to get the same numerical results as those obtained from the orbital frame of reference.

Formulation

The basic equations of motion, including the perturbations due to the Earth's oblateness and the atmospheric forces, are

$$\frac{d\boldsymbol{r}}{dt} = \boldsymbol{V} \tag{1a}$$

$$\frac{d\boldsymbol{V}}{dt} = \boldsymbol{g}(\boldsymbol{r}, \boldsymbol{V}) \tag{1b}$$

The vector $\boldsymbol{g} = \boldsymbol{F}_{2-\text{body}} + \boldsymbol{F}_{J_2} + \boldsymbol{D}$ is a function of both the radius vector and the velocity. The detailed expressions for the perturbations are the following:

$$\begin{aligned} \boldsymbol{F}_{2-\text{body}} &= -\mu \boldsymbol{r}/r^3 \\ \boldsymbol{F}_{J_2} &= \nabla_r \mathcal{R}_{J_2} \\ \boldsymbol{D} &= -K_D V \boldsymbol{V} \end{aligned} \tag{2}$$

where $K_D \overset{def}{=} \frac{1}{2}(A/m)\rho C_D$ and $\mathcal{R}_{J_2} = [(\mu J_2 R_E^2)/2r^3]\,[3(z^2/r^2) - 1]$ is the disturbing function related to the Earth's oblateness.

The linearized equations of motion have the form

$$\frac{d}{dt}\begin{Bmatrix}\delta \boldsymbol{r} \\ \delta \boldsymbol{V}\end{Bmatrix} = \mathbf{A}(t)\begin{Bmatrix}\delta \boldsymbol{r} \\ \delta \boldsymbol{V}\end{Bmatrix} \tag{3}$$

where

$$\mathbf{A} = \begin{pmatrix}\mathbf{0} & \mathbf{I} \\ \mathbf{G} & \mathbf{D}\end{pmatrix}, \qquad \mathbf{G} = \frac{\partial \boldsymbol{g}}{\partial \boldsymbol{r}}, \qquad \mathbf{D} = \frac{\partial \boldsymbol{g}}{\partial \boldsymbol{V}} \tag{4}$$

G corresponds to the gravity gradient matrix' and D will be named as the dissipation matrix. The two-body gravity gradient matrix is presented in Battin's book. Here, this matrix includes the J_2 terms as well as terms related to the variations of the atmospheric density. The dissipation matrix contains the atmospheric drag. Computing the gradients and denoting the unit dyadic as 1, we have

$$\frac{\partial \boldsymbol{g}}{\partial \boldsymbol{r}} = \frac{\mu}{r^5}[3\boldsymbol{r}\boldsymbol{r} - r^2\mathbf{1}] + \nabla_r \nabla_r \mathcal{R}_{J_2} + \frac{K_D V}{H}\boldsymbol{V}\boldsymbol{r} \tag{5}$$

where the last term reflects the density variation, assuming an exponential model:

$$\frac{\partial \boldsymbol{g}}{\partial \boldsymbol{V}} = -\frac{K_D}{V}[\boldsymbol{V}\boldsymbol{V} + V^2\mathbf{1}] \tag{6}$$

At this point we are ready for evaluating the volume. Let $\Phi_{12(t,t0)} = \partial \boldsymbol{r}/\partial \boldsymbol{V}_0$, then it can be shown* that the volume is the image of its initial value under the mapping Φ_{12}.

Received Jan. 2, 1993; revision received March 29, 1993; accepted for publication May 12, 1993.

*Aerospace Scientist, P.O. Box 606. Member AIAA.

We consider here the normalized volume[3] due to an isotropic explosion. The volume is related to the absolute value of the determinant of Φ_{12}. This partition (Φ_{12}) satisfies the matrix differential equations

$$\frac{d\Phi_{12}}{dt} = \Phi_{22} \tag{7a}$$

$$\frac{d\Phi_{22}}{dt} = -Ga_1, + \mathbf{D}a_n \tag{7b}$$

subject to the initial conditions: $\Phi_{12(t_0)} = \mathbf{0}$ and $\Phi_{22(t_0)} = \mathbf{I}$. A straightforward substitution of the solution for the combined system—Eqs. (3) and (7)—leads to the desired volume. It should be noted that the resulting volume is valid for a restricted magnitude of deviation from the nominal orbit, depending on the initial conditions and the nature of the perturbations.

Some Qualitative Properties of the Problem

It is generally impossible to provide an analytical closed-form solution for the volume. Although a numerical solution is a straightforward procedure, we wish to have some insight regarding the perturbations effects on the volume. For this purpose, we will examine some indirect properties of our problem.

The first are the four integrals of motion, the energy, and the angular momentum. The energy is perturbed by the drag, which causes a secular change while the oblateness is expressed in periodic changes. The angular momentum integrals, except one invariant corresponding to the oblateness, are perturbed by all of the forces. Now, the most distorted parts of the time history of the volume are the constriction points. Since the major distortion mechanism is the variation of the orbital rate, we expect the drag to be the most significant perturbation, for low altitude orbits.

A different point of view is by considering the volume in the phase space. It can be shown[8] that the volume propagates according to the Liouville's formula:

$$\mathrm{Vol}_{(t)} = \mathrm{Vol}_{(t_0)} e^{\mathrm{tr}\{A\}(t - t_0)} \tag{8}$$

The only nonzero trace of our system is $tr\{\nabla_V D\} = -4K_D V$. Thus, the volume in our case is

$$\mathrm{Vol}_{(t)} = \mathrm{Vol}_{(t_0)}\, e^{-4[K_D V](t - t_0)} \tag{9}$$

Hence, only the drag contributes to the secular change of the volume. The oblateness perturbations as well as the variations of the density are related to the gravity gradient matrix, therefore do not play any role in this discussion.

The final point of view is to consider the symplectic properties of the transition matrix': Φ is a symplectic matrix if

$$\Phi^T \mathbf{J} \Phi = \mathbf{J} \tag{10}$$

where

$$\mathbf{J} = \begin{pmatrix} \mathbf{0} & \mathbf{I} \\ -\mathbf{I} & \mathbf{0} \end{pmatrix} \tag{11}$$

Since $\Phi_{(t_0, t_0)}$ is symplectic, the time derivative of $\Phi^T \mathbf{J} \Phi$ should be zero, for $t > t_0$. It can be easily shown that

$$\frac{d}{dt}[\Phi^T \mathbf{J} \Phi] = \Phi^T \begin{pmatrix} \mathbf{G} - \mathbf{G}^T & \mathbf{D} \\ -\mathbf{D}^T & \mathbf{D} \\ & \mathbf{0} \end{pmatrix} \Phi \tag{12}$$

Now, $\nabla_r \boldsymbol{F}_{2\text{-body}}$ and $\nabla_r F_{J_2}$ are symmetrical and $\boldsymbol{D}$ is a nonzero matrix. Therefore, the J_2 perturbation keeps the symplectic structure of our system, while the atmospheric perturbations destroy it.

Orbital Debris Applications

The influence of the major perturbations on the volume of debris after an explosion is demonstrated here. A typical low near-circular orbit is chosen: a = 6678 km, e = 0.001, and i = 30 deg. The breakup occurs at the equator passage. In addition, the debris particles are considered very light for the purpose of a clear demonstration. In the following figures the dotted line represents the unperturbed (reference) volume, while the solid line is the perturbed one. Figure 1 shows the decrease of the volume due to the drag and also magnifies the constriction points. Although the latter have a time shifting (lead) because of the variation of the orbital rate, the nature of these points is clearly unchanged. The result is in a qualitative agreement with the prediction due to Liouville's theorem. The change of the volume is related to the trace of the system matrix. In our case, the trace is identical with the trace of the dissipation matrix, which is a negative quantity.

The influence of the Earth's oblateness on the volume is demonstrated via the volume residual (Fig. 2). Here, the dotted line represents the unperturbed volume whereas the solid line is the difference between the perturbed and the unperturbed volume. The residual has a periodic growing nature. The dominant frequency is twice the orbital rate which is the leading frequency of the J_2 short-period solution. A small time shifting in the one-dimensional constriction point, due to small changes

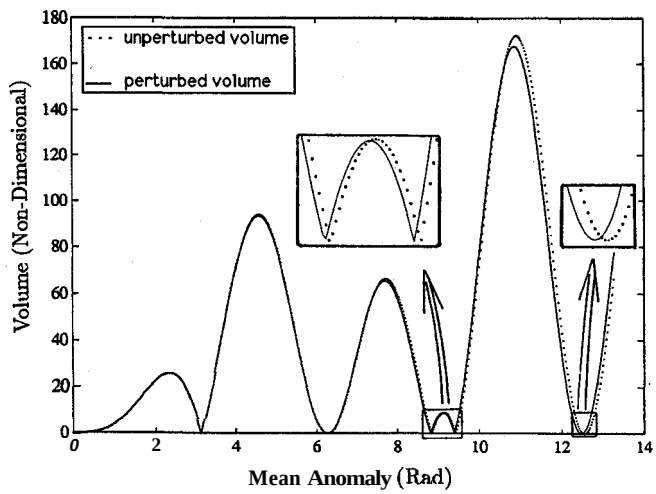

Fig. 1 Drag influence on the volume.

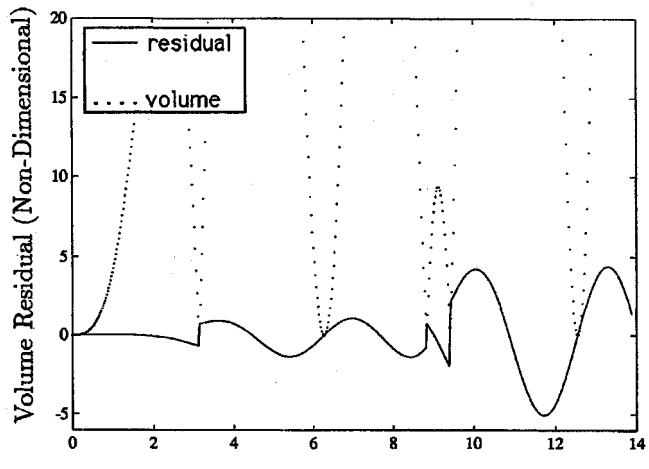

Fig. 2 $J2$ influence on the volume.

in the mean motion, is responsible for the sharp changes in the residual.

Remarks

This work presented the effects of the atmospheric drag and the Earth's oblateness on the volume of particles after an isotropic breakup. A special concern was given to the constriction points. The general nature of these points was not affected by the perturbations. However, it should be noted that the perturbations were considered as a field. It is sufficient for the J_2 part but is a limited particular model for the atmospheric perturbations. We have assumed this model because of its autonomous property. In other words, the perturbations here are an inherent part of the transition matrix as well as a part of the volume. Another way of modeling the atmospheric perturbations is by assuming a distribution of aerodynamic coefficients. This model cannot be handled by the current approach and may be carried out by using extensive numerical simulations for each particle.

References

[1] Jehn, R., "Dispersion of Debris Cloud from In-Orbit Fragmentation Events," *European Space Agency Journal*, Vol. 15, No. 1, 1991, pp. 63–77.

[2] Ashenberg, J., "On the Short-Term Spread of Space Debris," AIAA Paper 92-4441, Aug. 1992.

[3] Chobotov, V. A., "Dynamics of Orbiting Debris Cloud and the Resulting Collision Hazard to Spacecraft," International Academy of Astronautics, IAA-87-571, 1987.

[4] Jenkin, A. B., and Sorge, M. E., "Debris Cloud in Eccentric Orbits," AIAA Paper 90-3903, Sept. 1990.

[5] Ashenberg, J., "The Effect of the Earth's Oblateness on the Long-Term Dispersion of Debris," *Advances in Space Research* (to be published).

[6] Clohessy, W. H., and Wiltshire, R. S., "Terminal Guidance System for Satellite Rendezvous," *Journal of the Aerospace Sciences*, Vol. 27, Sept. 1960, pp. 653–658.

[7] Battin, R. H., *An Introduction to the Mathematics and Methods of Astrodynamics*, AIAA Education Series, AIAA, Washington, DC, 1987, pp. 450–455.

[8] Arnold, V. L., *Mathematical Methods of Classical Mechanics*, Springer-Verlag, Berlin, 1989, pp. 68–70.

Alfred L. Vampola
Associate Editor

Broadband Radio-Frequency Spectrum from Electrostatic Discharges on Spacecraft

H. C. Koons*
The Aerospace Corporation, Los Angeles, California 90009
and
T. S. Chin†
Lockheed Missiles & Space Company, Inc., Sunnyvale, California 94088

Introduction

VARIOUS aspects of the space environment can cause anomalous behavior of components on spacecraft. The plasma environment (especially around geosynchronous orbit) can differentially charge materials on the surface of a vehicle.[1–3] Spacecraft anomalies attributable to the resulting electrostatic discharges have been known to cause command errors, spurious signals, phantom commands, degraded sensor performance, part failure, and even complete mission loss.[4] Electromagnetic interference (EMI) from the resulting discharges may also interfere with communication systems on the spacecraft. Although many measurements of the properties of discharges have been made in space and in the laboratory, few have included the complete electromagnetic spectrum in the radio-frequency (RF) range. The purpose of this note is to compare new measurements of the RF spectrum from the Kapton blanket from the backside of the MILSTAR spacecraft's flexible substrate solar array (FSSA) with other space and laboratory data so that they will be more readily available for the analysis of spacecraft systems. The data may be used to estimate the effects of EMI from discharges on spacecraft systems operating in the frequency range from 100 kHz to 10 GHz.

Data

Figure 1 shows the broadband RF spectra of electrostatic discharges from 100 kHz to 10 GHz from a variety of different measurements. The original data have been converted to a standard distance of one meter. The MILSTAR flexible substrate solar array (FSSA) data were obtained from discharge measurements performed by Stanford Research Institute for Lockheed Missiles & Space Company, Inc. on a Kapton blanket sample from the backside of the solar array for the MILSTAR satellite. The blanket sample would cover eight solar cells arranged in a 2 × 4 array. The sample size was 15 × 30 cm (450 cm^2). About 20% of the Kapton blanket was covered on the inside by copper metallization. The data shown in Fig. 1 are from a series of tests on the sample at an electron beam energy of 20 keV and a beam current of 5 nA/cm^2. They are representative of the measurements at low frequency (LF), high frequency (HF), and uhf. The error brackets are drawn at ± 1 standard deviation for a sample of 14 or 15 discharges at each frequency.

The solid curve and the long-dashed curve are the spectra measured by Leung for two different-sized samples of Mylar.[5,6] The Mylar samples were irradiated by a 20-keV electron beam with a current density of 2–5 nA/cm^2. The peak pulse current was typically 150 A and the pulse width was 230 ns.

The measurement in Fig. 1 identified by the circle was made by the RF analyzer aboard the SCATHA spacecraft during a period when electron beam experiments were being performed on that vehicle? The RF analyzer measures electromagnetic emissions in the frequency range from 2 MHz to 30 MHz. The antenna for these measurements is an extendible 100-m, tip-to-tip dipole provided by the Goddard Space Flight Center for their dc-field experiment. The RF Analyzer can be operated in either a swept or a fixed-frequency mode. The design includes five frequency bands, two sweep rates, and two detection bandwidths. The signal amplitude is sampled 400 times per second, converted to an eight-bit digital format, and telemetered on a special purpose 3-kHz broadband data channel. During tape-recorded data collection, the amplitude is sampled 8 times per second. Only fixed frequency operation takes place in this mode. At the time the measurement in Fig. 1 was made, the RF analyzer was tuned to 20 MHz with a bandwidth of 4 kHz. The peak power was measured to be −83 dBm. It is not known what material was discharging. The electron beam was operating at 3 keV and 6 mA.

The dotted curve is the RF spectrum of a MIL-STD-1541A spark gap.[6] According to MIL-STD-1541A the spark gap is to be established at a level of 10 kV and the energy in the spark should be greater than 2×10^{-3} W-s.

The short-dashed curve is the spectrum measured by Wilson and Ma using a commercially available electrostatic discharge (ESD) simulator and a target: The target was an 8-mm-diam brass ball. For the spectrum shown in Fig. 1, the voltage was 4 kV. The peak current was 26 A with an approximate rise

Received March 4, 1993; revision received April 12, 1993; accepted for publication May 19, 1993.

*Senior Scientist, Space and Environment Technology Center, P. O. Box 92957. Member AIAA.

†Research Specialist, Space Systems Division, P. O. Box 3504.